ESR Studies of NO_2 Adsorbed on Surfaces. Analysis of Motional Dynamics

M. Shiotani[†] and J. H. Freed*

Baker Laboratory of Chemistry, Cornell University, Ithaca, New York 14853 *(Received: June 16, 1981)*

ESR spectra of NO_2 adsorbed on crushed Vycor glass and on a zeolite were observed in the temperature range 4.8–221 K. Based upon spectral simulations using the slow-motional ESR theory for different models of rotational diffusion, we found that for NO_2 motion on the Vycor surface the following occurs: (1) At 4.8 K, NO_2 still shows residual motional effects. (2) Below 77 K the rotational motion of NO_2 is axially symmetric about the y axis (i.e. parallel to the O–O internuclear axis) such that $N \equiv R_\parallel/R_\perp \approx 10$. The parallel component of the diffusion tensor, $R_\parallel$, increases with temperature, e.g., $R_\parallel = 5 \times 10^5$ and 1×10^7 s^{-1} at 4.8 and 77 K, respectively (based on a Brownian diffusion model). (3) Above 77 K, $R_\perp$ increases with temperature so that almost isotropic rotational diffusion is estimated at 185 K (i.e., $R_\parallel = 1 \times 10^7$ s^{-1} and $N = 1.3$), presumably due to a translational diffusion mechanism. (4) There are discrepancies between the observed and calculated line shapes especially for $T \lesssim$ 77 K. None of the models used could improve the agreement, and possible improvements of the models are outlined. A quantum mechanical analysis of the 4.8 K spectrum implies either a renormalized moment of inertia for NO_2 that is orders of magnitude greater than that in the gas phase and/or a strong orientation-dependent interaction potential with the surface. In either case it is suggested that the y axis should be parallel to the surface. Additional line broadening probably due to an exchange process modulated by translational diffusion rapidly increases with temperature above 77 K, even though the NO_2 surface concentration decreases with increasing temperature. Distinct differences in motional dynamics are observed for NO_2 on the zeolite support.

Introduction

Nitrogen dioxide, NO_2, a stable paramagnetic gaseous molecule has been studied by a number of investigators using ESR.[1-14] The ESR parameters and their relation to the electronic structure have been well established from single-crystal studies[1,3,4] and molecular orbital calculations.[15-17] The ESR parameters reported are summarized in Table I and the molecular coordinates related to the magnetic parameters are shown in Figure 1. Thus, NO_2 has potential as a "spin probe" for the study of molecular dynamics at the gas–solid interface by ESR.

In the course of our recent study of reactions between NO_2 and Cu–metal supported on porous Vycor glass,[18] it was also found that the NO_2 adsorbed on the Vycor gave strongly temperature-dependent ESR spectra. We therefore decided to study NO_2 on the pure Vycor for a molecular-dynamics study in order to eliminate the background signal from the Cu^{2+}–NO_2 complexes.

Although there have been ESR studies of molecular motion of NO_2 in the adsorbed state[9,11,19] and in solid media,[4,20-22] most of these studies were limited to *qualitative* analysis of the spectra. Only one paper, on the motional dynamics of NO_2 in synthetic zeolites, by Pietrzak and Wood[9] attempts a quantitative analysis. They analyzed their temperature-dependent ESR line shapes using an early approximate theory[23] and concluded that there was no preferred axis of rotation for the NO_2. However, our temperature-dependent NO_2 spectra are considerably different in appearance from those of the NO_2/zeolite system,[9] but very similar to those from NO_2/silica gel.[11]

In our laboratory, the theory for slow-motional ESR spectra has been extensively developed and has been applied successfully to ESR line shapes of nitroxides and the VO^{2+} ion in isotropic and anisotropic liquids.[24-28] Recently, the theory was applied to the analysis of the temperature-dependent ESR line shapes of O_2^- adsorbed on Ti ions supported on Vycor glass, and it was concluded that the motion of O_2^- on the surface was highly anisotropic, consisting essentially of planar rotation about the axis perpendicular to the internuclear axis of O_2^- and parallel to the normal to the surface.[29] We thus showed that our theory for slow-motional ESR spectra is very useful in the study of molecular dynamics at the gas–solid interface.

[†] Faculty of Engineering, Hokkaido University, Sapporo 060, Japan.

(1) H. Zeldes and R. Livingston, *J. Chem. Phys.*, **35**, 563 (1961).
(2) J. Tateno and K. Gosi, *J. Chem. Phys.*, **40**, 1317 (1964).
(3) W. C. Mosley and W. G. Moulton, *J. Chem. Phys.*, **43**, 1207 (1965).
(4) H. Zeldes, *Paramagn. Resonan., Proc. Intern. Conf., 1st, 1962*, **2**, 264 (1963).
(5) P. W. Atkins, N. Keen, and M. C. R. Symons, *J. Chem. Soc.*, 2873 (1962).
(6) C. Chachaty, *J. Chim. Phys.*, **62**, 728 (1965).
(7) T. J. Schaafsma, G. A. V. D. Velde, and J. Kommandeur, *Mol. Phys.*, **14**, 501 (1968).
(8) P. H. Kasai, W. Weltner, Jr., and E. B. Whipple, *J. Chem. Phys.*, **42**, 1120 (1965).
(9) T. M. Pietrzak and D. E. Wood, *J. Chem. Phys.*, **53**, 2454 (1970).
(10) R. D. Iyenger and V. V. Subba Rao, *J. Am. Chem. Soc.*, **90**, 3267 (1968).
(11) M. Iwaizumi, S. Kubota, and T. Isobe, *Bull. Chem. Soc. Jpn.*, **44**, 3227 (1971).
(12) G. R. Bird, J. C. Baird, A. W. Jache, J. A. Hodgson, R. F. Curl, A. C. Kunkle, J. W. Brandsford, J. Rastrup-Anderson, and J. Rosenthal, *J. Chem. Phys.*, **40**, 3378 (1964).
(13) J. H. Lunsford, *J. Colloid Interface Sci.*, **26**, 355 (1968).
(14) P. H. Kasai and R. J. Bishop, *ACS Monogr.*, **No. 171**, 350 (1976).
(15) R. S. Mulliken, *Rev. Mod. Phys.*, **14**, 204 (1942).
(16) K. L. McEwen, *J. Chem. Phys.*, **32**, 1801 (1960); **34**, 547 (1961).
(17) M. Green and J. W. Linnett, *Trans. Faraday Soc.*, **57**, 1 (1961).
(18) M. Nilges, M. Shiotani, C. T. Yu, G. Barkley, Y. Kera, and J. H. Freed, *J. Chem. Phys.*, **73**, 588 (1980).
(19) C. B. Colburn, R. Ettinger, and F. A. Johnson, *Inorg. Chem.*, **2**, 1305 (1963).
(20) T. J. Schaafsma and J. Kommandeur, *Mol. Phys.*, **14**, 517 (1967).
(21) J. R. Brailsford and J. R. Morton, *J. Magn. Reson.*, **1**, 575 (1969).
(22) I. Bojko and R. H. Silsbee, *J. Magn. Reson.*, **5**, 339 (1971).
(23) M. S. Itzkowitz, *J. Chem. Phys.*, **46**, 3048 (1967).
(24) S. A. Goldman, G. V. Bruno, C. F. Polnaszek, and J. H. Freed, *J. Chem. Phys.*, **56**, 716 (1972).
(25) J. H. Freed, "Spin Labelling: Theory and Applications", L. Berliner, Ed., Academic Press, New York, 1976, Vol. 1, Chapter 3.
(26) J. S. Hwang, R. P. Mason, L. P. Hwang, and J. H. Freed, *J. Phys. Chem.*, **79**, 489 (1975).
(27) C. F. Polnaszek and J. H. Freed, *J. Phys. Chem.*, **79**, 2283 (1975).
(28) R. F. Campbell and J. H. Freed, *J. Phys. Chem.*, **84**, 2668 (1980).
(29) M. Shiotani, G. Moro, and J. H. Freed, *J. Chem. Phys.*, **74**, 3757 (1981).

0022-3654/81/2085-3873$01.25/0

TABLE I: ESR Parameters of NO_2 in Various Media

medium	g values				hyperfine interaction, MHz				ref
	g_x	g_y	g_z	g_{iso}	A_x	A_y	A_z	a_{iso}	
$NaNO_2$[a] (77 K)	2.0057	1.9910	2.0015	1.9994	138.4	130.9	190.2	153.2	1
$NaNO_2$[a] (293 K)	2.0059	2.0052	2.0055	2.0055	102.2	92.7	140.3	111.7	2
$AgNO_3$[a] (77 K)	2.0090	1.9978	2.0039	2.0036	143.1	135.1	195.3	157.8	3
KNO_3 (77 K)	2.0055	1.9932	1.9996	1.9994	136.6	141.1	176.3	151.3	4
ice (77 K)	2.0066	1.9920	2.0022	2.0003	141.6	139.6	196.8	159.3	5
CH_3NO_2 (77 K)	2.0047	1.9915	2.0011	1.9991	132.6	124.3	182.4	146.4	6
N_2O_4 (77 K)	2.0054	1.9913	2.0015	1.9994	140.9	134.8	188.2	154.6	7
neon (4 K)	2.0062	1.9920	2.0030	2.0004	145.2	127.7	173.0	148.6	8
zeolite (Ca-X)[b] (114 K)	2.0051	1.9921	2.0017	1.9996	145.7	133.3	189.4	156.1	9
zeolite (Na-X)[b] (77 K)	2.0043	1.9922	2.0015	1.9993	143.3	137.2	189.1	156.5	9
ZnO[b] (77 K)	2.007	1.994	2.003	2.001	146.1	132.0	181.1	153.1	10
silica gel[b] (77 K)	(2.004)[c]	1.9907	(2.004)[c]	1.9996	(165.7)[c]	137.0	(165.7)[c]	156.1	11
MgO (93 K)	2.005	1.9915	2.002	1.9995	148	137.0	189.0	158.0	13
NO_2[d,e] (gas) (293 K)	2.006178	1.991015	2.00199	1.9997	127.8	126.0	185.0	146.5	12
Vycor[b] (4.8 K)	2.0051	1.9913	2.0017	1.9994	140.3	128.2	183.5	150.7	f
zeolite (4.8 K) (Na-Zeolon (Norton))[b]	2.0051	1.9913	2.0017	1.9994	140.3	128.2	183.5	150.7	f

[a] Single-crystal studies. [b] Adsorbed state. [c] Averaged value of x and z components. [d] Microwave study. [e] The x, y, and z components of the quadrupole coupling tensor were found to be 0.9, 1.62, and −2.6 MHz or of negligible importance for ESR spectra. [f] Present work.

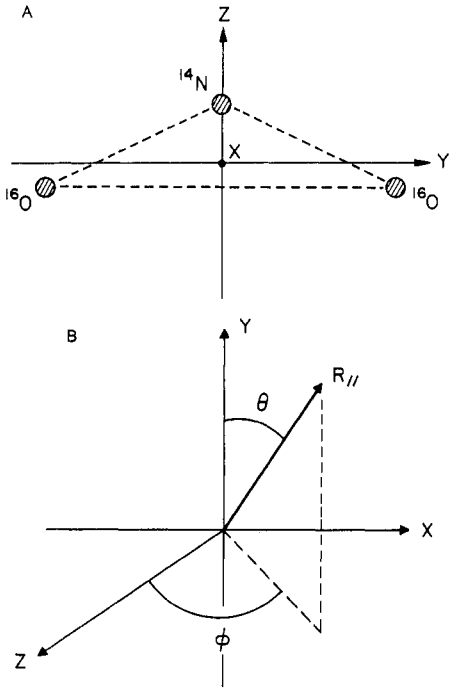

Figure 1. (a) Structure of $^{14}N^{16}O_2$. (b) Illustration of the geometry for NO_2 showing the case in which the principal diffusion axis is not necessarily coincident with the principal axes of the NO_2 **g** and **A** tensors.

We have found that NO_2 adsorbed on pure porous Vycor glass gives rise to strongly temperature-dependent ESR spectra over the temperature range 4.8–220 K. The purpose of the present paper is to discuss models for the motion of NO_2 on a Vycor surface which are consistent with the observed temperature-dependent ESR line shapes and to infer from this the dynamical structure of the adsorption site.

We first summarize our results on temperature-dependent ESR line shapes for NO_2 on Vycor. Then, these results are analyzed by detailed spectral simulation with the use of our slow-motional ESR spectral theory for different rotational diffusion models:[24,25] Brownian diffusion, jump diffusion, and approximate free diffusion. It will be shown that at low temperatures the rotational motion of NO_2 is primarily a rotation about the y axis (i.e., parallel to the internuclear axis between the oxygen atoms), but above 77 K the motion becomes nearly isotropic.

II. Experimental Section

(A) *Sample Preparation.* The porous Vycor quartz glass (Corning Code No. 7930, controlled pore size of 40 Å) was supplied in a crushed form by Dr. Jan Schreuers, Corning Glass Works. The cryshed Vycor was cleaned and activated in the manner described previously.[29,30]

The NO_2 used was obtained commercially (Madison Gas Products) and was purified by vacuum distillation. This gas gave the same results as NO_2 that was further purified by mixing with oxygen to remove NO. The equilibrium for the reaction $NO_2 \rightleftharpoons NO + {}^1/_2O_2$ is such that small amounts of NO and O_2 are always present in NO_2 and ESR signals due to O_2 gas are clearly observed at room temperature ($K_{298\,K} = 7.2 \times 10^{-7}$).[31]

The Vycor was exposed to about 10 torr of NO_2 (actually an equilibrium mixture of NO_2) at room temperature for several hours and then degassed briefly (ca. 1 min) to remove nonadsorbed NO_2 at the same temperature. The adsorbed NO_2 is physisorbed, since pumping for about 30 min results in a complete loss of ESR signal. Na–Zeolon (Norton)[32] was supplied by Dr. Paul H. Kasai, IBM. The zeolite was activated at 550 °C for 12 h under vacuum of $P \simeq 10^{-6}$ torr. About 500 torr of NO_2 was admitted to the zeolite at room temperature, and ESR spectra were recorded for the sample without degassing. Such high pressures were required in order to obtain an ESR signal, thus clearly demonstrating that the NO_2 is very weakly adsorbed on the zeolite.

(30) (a) R. B. Clarkson and A. C. Cirillo, Jr., *J. Vac. Sci. Technol.*, **9**, 1073 (1972); (b) *J. Catal.*, **33**, 392 (1974).

(31) This equilibrium constant was calculated by using the standard free enthalpy for the ideal gas reaction. Note that J. H. Lunsford has discussed the equilibrium between NO and O_2 gases and also the decomposition of NO_2 into NO and O_2 gases on an MgO surface (see ref 13).

(32) A kind of zeolite, sometimes called "mordenite". A typical unit contains $Na_{8.7}[(AlO_2)_{8.7}(SiO_2)_{39.3}\cdot 24H_2O]$, variation of Si/Al = 4.5∼5. The size of channel is around 9 Å (no large cavities except the channel).

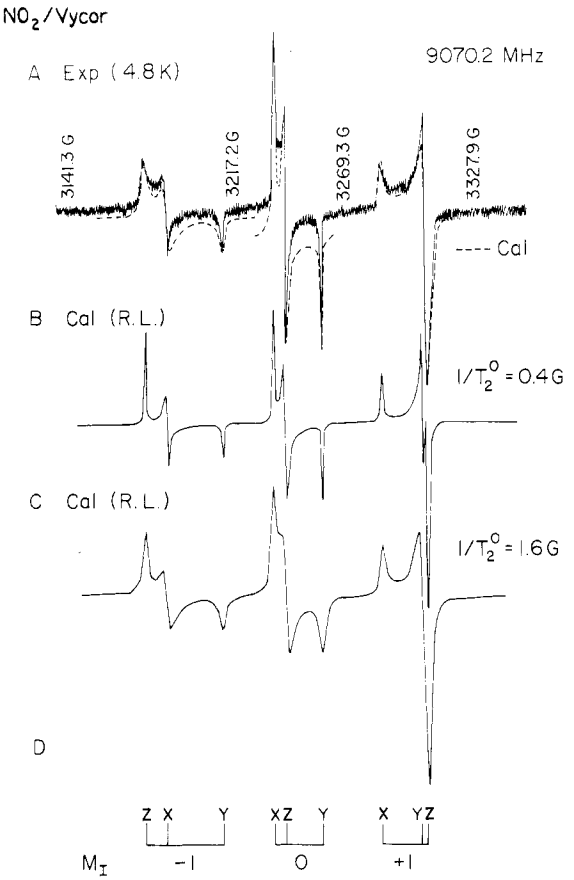

Figure 2. Experimental spectrum of NO_2 adsorbed on Vycor at 4.8 K (A) and spectra (B and C) calculated by the rigid-limit simulation program in order to determine the **A** and **g** tensor components precisely. Spectra B and C best fit the observed one at the band corresponding to $M_I = 0$ and the x, z components of $M_I = \pm 1$, respectively, with parameters $g_x = 2.0051$, $g_y = 1.9913$, $g_z = 2.0017$, $A_x = 50.0$ G, $A_y = 46.0$ G, $A_z = 65.5$ G, and Lorentzian line shape. Line widths of $1/T_2^0 = 0.4$ and 1.6 G were used for B and C, respectively. The dotted lines in A correspond to calculated line shape of B at $M_I = 0$ and C at the $M_I = \pm 1$ bands.

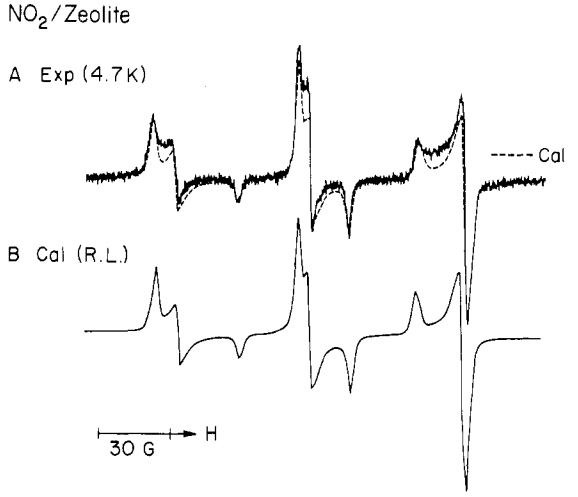

Figure 3. Experimental spectrum of NO_2 in zeolite (Na–Zeolon) at 4.7 K (A) and best fitting one (B) calculated by using the rigid-limit program. The **A** and **g** tensor components used are the same as those of NO_2–Vycor, but a Lorentzian line width of $1/T_2^0 = 1.2$ G was used.

(*B*) *Measurement of ESR Spectra.* ESR spectra were recorded at X-band with a Varian E-12 ESR spectrometer by employing 100-kHz (or 10-kHz when needed) field modulation at a low enough amplitude that no line shape distortion was observed. Microwave power was always adjusted so that no saturation occurred.

The sample temperature above 77 K was controlled by a Varian E-257 variable-temperature unit and measured with a copper–constantan thermocouple placed just above the sample. Moreover, the temperature of the sample was regulated within ±0.5 K between 4.2 and 80 K by means of an Oxford Instrument, ESR 9 continuous He gas flow cryostat.

The magnetic field was measured and calibrated with a Harvey-Wells gauss meter. The microwave frequency was measured with a Systron Donner electronic counter.

Relative spin concentrations at the different temperatures were determined by double integration of the experimental spectra after checking that the sensitivity remained unchanged. A Curie–Weiss law was assumed for the paramagnetic susceptibility.

III. Experimental Results and Analysis

(*A*) *Determination of* **A** *and* **g** *Tensor Components.* A number of ESR studies on NO_2 have been reported and the assignment of **A** and **g** tensor components has been well established by comparison with molecular orbital calculations.[15-17] However, the numerical values of **A** and **g** are considerably shifted from medium to medium as seen in Table I. Thus, in order to simulate slow-motional spectra of NO_2, one must first know the precise value of the **A** and **g** tensor components in the rigid limit for the present system.

The lowest temperature of our measurements was 4.8 K and the spectrum obtained is shown in Figure 2A. The simulation was carried out to accurately determine the ESR parameters of the spectrum at 4.8 K by using a rigid-limit simulation program. The best-fit theoretical spectra are shown in parts B and C of Figure 2, the difference between two theoretical spectra being only the intrinsic Lorentzian line width, $1/T_2^0$, used for the calculation. We show with a dotted line in Figure 2A that, to simulate the line shape corresponding to the x and z components at $M_I = \pm 1$, $1/T_2^0 = 1.6$ G is needed, but the line shape at $M_I = 0$ is well simulated by using $1/T_2^0 = 0.4$ G. Moreover, it is seen from Figure 2A that the experimental line width of the y component at $M_I = -1$ is less than that of the x and z components of $M_I = -1$, i.e., close to $1/T_2^0 = 0.4$ G. Thus, we find that the spectrum at 4.8 K cannot be simulated by a single line width, but the line width depends considerably on both the orientation and the value of M_I.

However, as shown in parts A and B of Figure 3, the spectrum of NO_2 adsorbed on zeolite at 4.7 K is simulated satisfactorily by use of a single line width and the same **A** and **g** tensor components as those of the NO_2/Vycor system.

These results indicate that even at 4.8 K the NO_2 on Vycor is not in the true rigid limit, but rather in an incipient slow-motional state. Nevertheless, the measured **A** and **g** tensor components should be very close to the rigid-limit values because of the following reasons. (1) The variation of the measured **A** and **g** components vs. temperature is shown in Figure 5. From this plot one can see that, below 11 K, the components no longer shift with temperature. (2) The greater sensitivity of the line widths, vs. the shifts in position, to motional effects is well-known in magnetic resonance (NMR and ESR) spectra,[33] since the lines first broaden before they shift.

Thus, we will use the **A** and **g** tensor components $A_x = 140.3$ MHz (50.0 G), $A_y = 128.2$ MHz (46.0 G), $A_z = 183.5$

(33) R. P. Mason and J. H. Freed, *J. Phys. Chem.*, 78, 1321 (1974).

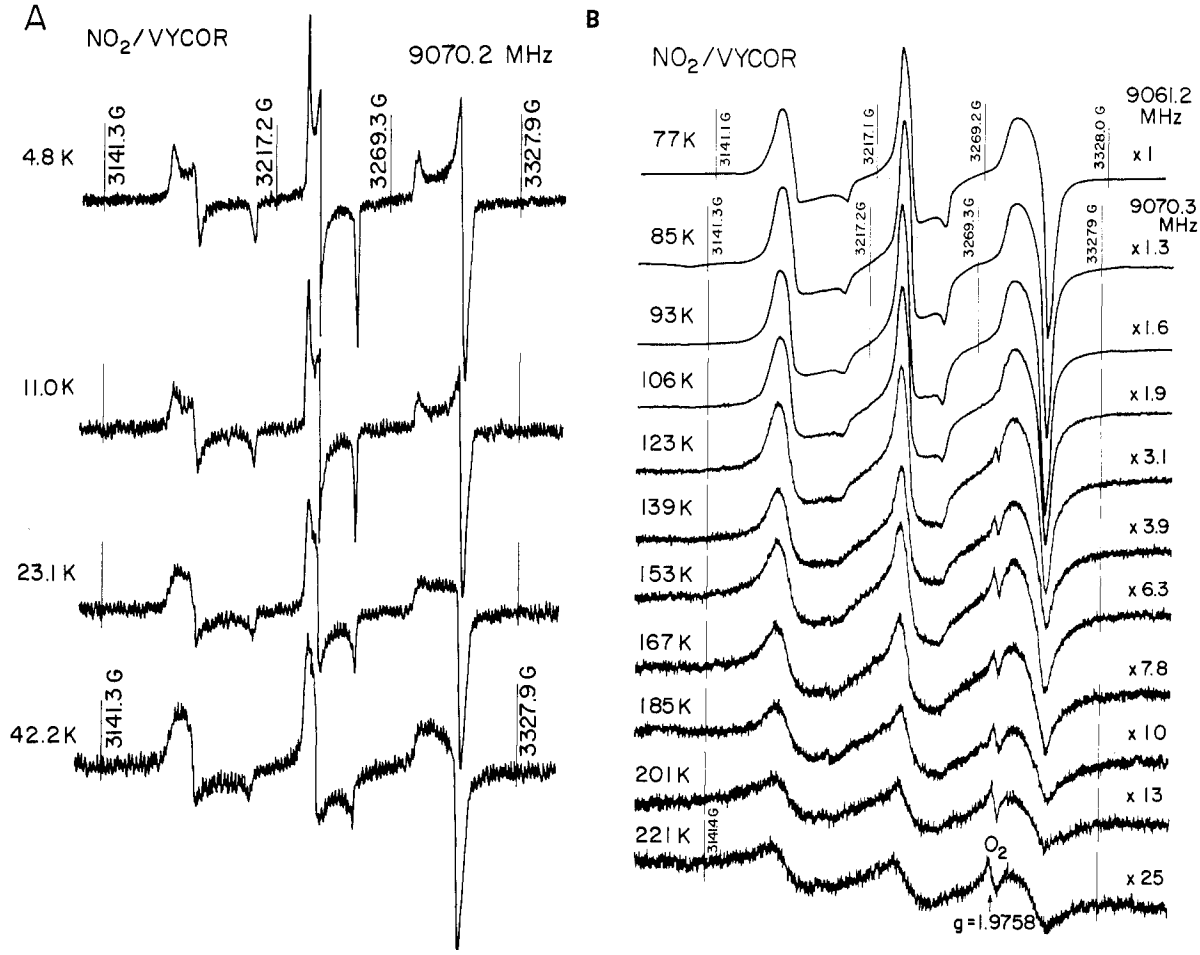

Figure 4. Temperature-dependent ESR spectra of NO_2–Vycor: (A) below 42.2 K; (B) above 77 K.

MHz (65.5 G), $g_x = 2.0051$, $g_y = 1.9913$, and $g_z = 2.0017$ for NO_2 at 4.8 K as the rigid-limit values in the following calculations.

The following three points should be noted about the present values of ESR parameters. (1) Schaafsma et al.[7] have pointed out that the contribution of the nonsecular terms of the spin Hamiltonian cannot be neglected because of the magnitude of the ^{14}N hyperfine splitting (i.e., second-order effects amount to a correction of about 0.5 G in the resonance position of the spectral lines and to about 5×10^{-4} in g values).[7] Therefore, second-order perturbation effects were taken into account in the spin Hamiltonian. It was found from the simulation that, although the line positions were shifted by the second-order contribution, the line shape was essentially unaffected when a line width larger than 0.4 G was used. (2) The present **g** components are very close to those reported for NO_2 trapped in a single crystal of $NaNO_2$[2] and in N_2O_4 medium[7] (see Table I). However, the **A** components are slightly different from the values reported for the above two studies. This might be explained by the NO_2 geometry, e.g., the bond angle of ONO, might be modified by the surface.[34] These and related matters are discussed more fully in section IV.

(B) Temperature-Dependent Spectra of NO_2 on Vycor Surfaces. The observed spectra in the temperature range from 4.8 to 221 K are shown in Figure 4. One can see that the line shape of the spectra depend strongly on temperature. In this section, we summarize the main characteristics of these spectra (cf. parts A and B of Fig 4[35] and the graph of resonance line position vs. temperature Figure 5). (1) Below 11 K, no line positions are shifted, but the line shape changes significantly between 4.8 and 11.0 K, i.e., the relative heights for the y components at $M_I = -1$ and 0 and for all components of the $M_I = 0$ band become weaker at 11 K. This change can be interpreted as a motional effect as noted in the previous section. (2) With further increase in temperature, the x and z components are gradually shifted toward their common center for all three M_I bands and then they collapse to one broad band at about 77 K. Below 77 K, although the line positions corresponding to the y component are also shifted from the original position toward the position corresponding to rapid isotropic motion (giving averaged values of **A** and **g** components), the degree of shift is much less than that of the x and y components (see especially, the $M_I = -1$ band). This fact indicates that the rate of rotational diffusion about the y axis (O ··· O direction, cf. Figure 1) is much greater than that about x and z axes in this tem-

(34) The ONO angle can be calculated by use of Coulson's relationship (C. A. Coulson, Victor Henri Commemoratif, Contribution a l'Etude de la Structure Moleculaire, 1948, p 15). The estimated bond angles are given in ref 7 for the NO_2 in a variety of matrices. The estimated angle (of 132°) for the present NO_2 adsorbed on vycor is slightly smaller than that for the gas phase (134°).

(35) (a) We also note the ESR signal due to gaseous O_2 at $g = 1.9758$ shown in Figure 4B (cf. ref 13). This identification was clearly confirmed by observation of an identical signal after admitting pure O_2 gas into a blank ESR sample tube. Nonobservation of this signal below around 100 K is probably due to either adsorption of O_2 onto the Vycor or a shift of the equilibrium constant for $NO_2 \rightleftharpoons NO + {}^1/_2O_2$ to the left. The same O_2 signal appears in the NO_2/MgO system reported by Lunsford[13] although he did not point it out (cf. the −180 °C spectrum in Figure 4a of ref 13). (b) Note also that the line shape of NO_2 on MgO (at −180 °C)[13] is close to the one we observed at 23.1 K. on Vycor.

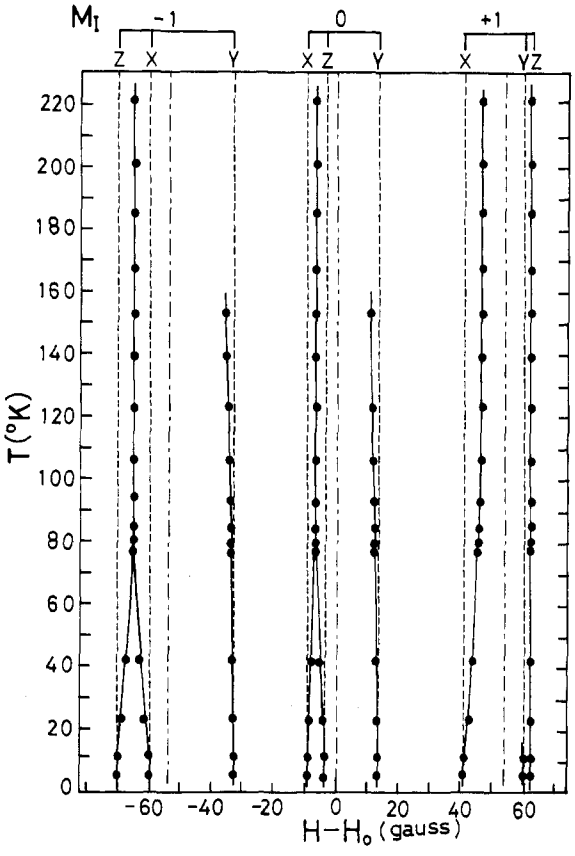

Figure 5. Plot of experimental resonance positions vs. temperature. H_0 stands for a magnetic field strength of 3241.0 G. A microwave frequency of ν = 9.070 GHz was used. The lines (····) and (−·−·−) stand for the resonance line positions corresponding to the rigid limit and to the fast isotropic motion, respectively (see the text for details).

perature range. (3) Above 77 K, the positions of the collapsed lines from the x and z components are almost unchanged, but the y components (at the M_I = −1, 0 bands) are seen to shift to the central part. This fact indicates that, in this temperature range, the rotational motion about the y axis increases significantly. (4) The M_I = +1 band is not consistent with the observations on the M_I = −1 and 0 bands. That is the y component for M_I = +1 is not visible, while the position of the z component for M_I = +1 appears to be almost constant with temperature. (5) The line positions of the y component gradually become more diffuse with increasing temperature and are undetectable above 153 K. This may reflect increased rotational motion about the x and z axes and also the increased line width with temperature. The increase of the observed line width can be explained partly by the increase of rotational motion, but another mechanism for line broadening should also be considered. These matters will be discussed in detail in section D. (6) Another important observation is that the signal intensity of NO_2 determined by double integration decreased considerably with increasing temperature. For example, the concentration of NO_2 at 221 K is about 4% that at 77 K.[36]

Finally, it should be noted that the present spectra of NO_2 observed over a wide temperature range are completely different from those in the gas phase,[37-39] but characteristic of adsorbed species on the solid surface or trapped species in the solid matrix.

(36) The equilibrium constant K_p = 0.14 ± 0.02 has been measured by Nordstrom and Chan [*J. Phys. Chem.*, **80**, 847 (1976)] for $N_2O_4 \rightleftharpoons 2NO_2$. This is very close to the value 0.146 calculated in the ideal gas approximation where $\Delta G_f°_{298}$ = 1.14 kcal/mol. While at pressures below 1 torr and 298 K nearly all the NO_2 in the gas phase is dissociated, at 1 atm only about 1/3 mole fraction is. Enhanced dimerization on the Vycor surface with increasing temperature would require a $\Delta G_f°_{298}$ that is negative for the *surface*.

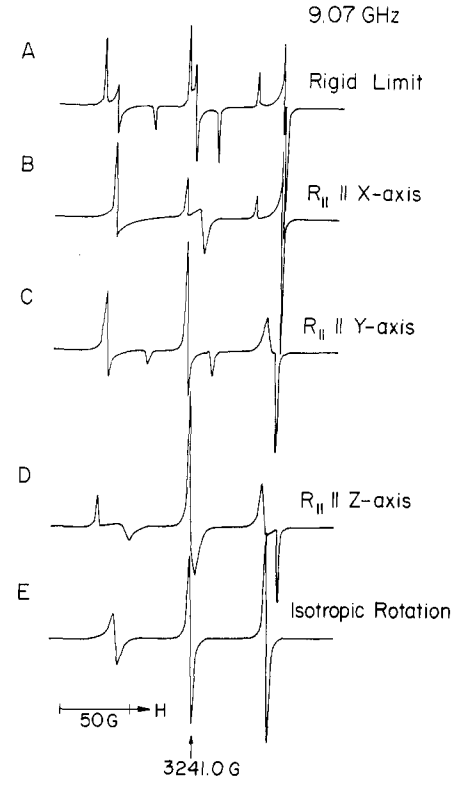

Figure 6. Theoretical spectra of NO_2 rotating about its x axis (B), y axis (C), and z axis (D). The spectra were calculated for Brownian rotational diffusion model by using $R_{\parallel}$ = 1 × 10^8 s^{-1}, $R_{\perp}$ = 5 × 10^5 s^{-1}, and $1/T^0$ = 0.4 G. For isotropic rotation (E), $R_{\parallel}$ = $R_{\perp}$ = 1 × 10^8 s^{-1} was used.

(C) *Spectral Simulations.* The spectral simulations of the temperature-dependent ESR spectra were carried out by using our slow-motional ESR simulation theory (programmed for a PDP-11 computer), for the rotational models:[24,25] Brownian diffusion, jump diffusion (from weak to strong jump), and approximate free diffusion.

Note that for anisotropic rotational diffusion, the eigenvalues $E_{L,K}$ of the diffusion operator are given by the expression

$$E_{L,K} = R_{\perp}B_L{}^{\perp}L(L+1) + (R_{\parallel}B_K{}^{\parallel} - R_{\perp}B_K{}^{\perp})K^2$$

where $B_L{}^{\perp} = [1 + R_{\perp}\tau_{\perp}L(L+1)]^{-p}$ and $B_K{}^{\sigma} = [1 + R_{\sigma}\tau_{\sigma}K^2]^{-p}$ (σ = ∥ or ⊥) and p = 1 for jump diffusion and p = 1/2 for approximate free diffusion. The definitions of L, K, $\tau_{\parallel}$, and $\tau_{\perp}$ are given elsewhere,[25] but we note that the magnitude of $R_{\perp}\tau_{\perp}$ or $R_{\parallel}\tau_{\parallel}$ is a measure of the mean jump size (or approximate inertial effect). Simple Brownian diffusion is obtained by letting $R_{\perp}\tau_{\perp}$ and $R_{\parallel}\tau_{\parallel} \rightarrow 0$ so $B_L = B_K = 1$. In the present paper, for the purpose of comparing different models, anisotropic rotational correlation times, $\tau_{R\parallel}$, $\tau_{R\perp}$ and isotropic rotational correlation time τ_R are defined as

$$\tau_{R\parallel} = (4\,R_{\parallel}B_2{}^{\parallel})^{-1} \qquad \tau_{R\perp} = (6R_{\perp}B_2{}^{\perp})^{-1}$$

$$\tau_R = (\tau_{R\parallel}\tau_{R\perp})^{1/2}$$

(37) G. Castle and R. Beringer, *Phys. Rev.*, **80**, 114 (1950).
(38) T. J. Schaafsma, *Chem. Phys. Lett.*, 1, 16 (1967).
(39) O. S. Burch, W. H. Tanttila, and M. Mizushima, *J. Chem. Phys.*, **61**, 1607 (1974).

respectively. Furthermore, in order to study any line shape features due to the orientation of the main principal axis about which rotational diffusion occurs,[40] we varied the polar angles (θ and ϕ) (cf. Figure 1B) which define the orientation of this axis relative to the coordinate system determined by the principal axes of the NO_2 **g** and **A** tensors.

The theoretical spectra shown in Figure 6 were calculated with a Brownian rotational diffusion model in order to demonstrate how the line shape varies when the molecular axis about which rapid rotation takes place is changed from the z to x or y axis (cf. parts A and B of Figure 1). For the calculation, highly anisotropic motion of $N \equiv R_\parallel/R_\perp = 200$ was assumed, with $R_\perp = 5 \times 10^5\ s^{-1}$ and $R_\parallel = 1 \times 10^8\ s^{-1}$. Note that $R_\perp = 5 \times 10^5\ s^{-1}$ is a small enough value that it causes only a slight line broadening, and not any significant line position shift. However, $R_\parallel = 1 \times 10^8\ s^{-1}$ corresponds to motional narrowing in which tensor components perpendicular to the rotation axis are completely averaged out. For example, in the case of $R_\parallel \parallel y$ axis (Figure 6C), it is seen that, although the line corresponding to the y component remains at its rigid-limit position, the x and z components are averaged out and the line width of the y component becomes slightly broader. In the case of $R_\parallel \parallel z$ axis (Figure 6B), the x and y component are again averaged out, but the degree of broadening of the collapsed line is seen to be different at each M_I band. The latter can be understood by recognizing that the degree of line broadening is related to $R_\parallel$ and the separation frequency between the two components. In the case of $R_\parallel \parallel x$ (Figure 6C), the same type of argument again applied. The experimental spectra are clearly consistent with the case that $R_\parallel \parallel y$, especially in the lower temperature region.

Changes in the theoretical line shape occurring as a function of $R_\parallel$ are shown in Figure 7. The sensitivity of the ESR line shape to molecular motion is seen from close to the rigid limit to the motionally narrowed region, and with $R_\perp$ held constant at a small (rigid-limit) value.

The characteristics derived from the theoretical spectra are summarized as follows. (1) First, we note that, for $R_\parallel \leq 2.5 \times 10^6\ s^{-1}$ and $R_\perp \leq 2.5 \times 10^5\ s^{-1}$, the position of each line is found to be essentially unshifted, but the line shape is changed slightly with decreasing $R_\parallel$. (2) In the slow-motional region ($R_\parallel \simeq 2.5 \times 10^6\ s^{-1}$), the lines due to **A** and **g** anisotropies are well separated. With increasing $R_\parallel$, the doublet of x and y components is shifted to the common center. Around $R_\parallel = 1 \times 10^7\ s^{-1}$, the doublet at the $M_I = 0$ band becomes one broad line, whereas those at the $M_I = \pm 1$ bands are still separated. The doublets at the $M_I = -1$ and $+1$ bands collapse around $R_\parallel = 2.5 \times 10^7\ s^{-1}$ and $R_\parallel = 5 \times 10^7\ s^{-1}$, respectively. (3) It is also seen that the collapsed line width becomes narrower with further increase in $R_\parallel$, i.e., the relative peak height compared with that of the y component is greater. The line broadening of the y component is almost negligible with increasing $R_\parallel$, which is reasonable since $R_\parallel \parallel y$ axis. (4) Another important feature of the theoretical spectrum is the relative peak heights at different M_I bands, i.e., the peaks of the y, z components at the $M_I = \pm 1$ bands are the highest for $R_\parallel \leq 1 \times 10^7\ s^{-1}$, but that at the $M_I = 0$ band gradually increases for $R_\parallel \geq 1 \times 10^7\ s^{-1}$ and becomes greater than the one at $M_I = \pm 1$ for $R_\parallel = 5 \times 10^7\ s^{-1}$.

Next, the contribution of $R_\perp$ to the line shape for the Brownian diffusion model is considered. Theoretical spectra were calculated as a function of $R_\perp$. A value of

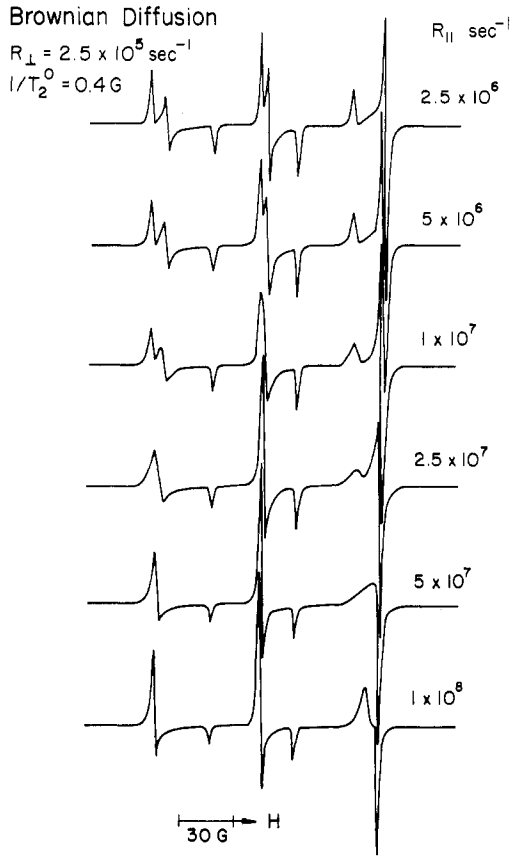

Figure 7. Theoretical spectra illustrating the change in the line shape occurring as a function of $R_\parallel$ (parallel to y axis) for anisotropic Brownian rotational diffusion. Here, $R_\perp = 2.5 \times 10^5\ s^{-1}$ and the intrinsic line width of $1/T_2^0 = 0.4$ G.

$R_\parallel = 1 \times 10^7\ s^{-1}$ was used (corresponding to intermediate slow motion), while $R_\perp$ was varied from $R_\perp = 2.5 \times 10^5$ to $1 \times 10^7\ s^{-1}$. For $R_\perp \leq 1 \times 10^6\ s^{-1}$, the line shape remains unchanged. For $R_\perp \geq 1 \times 10^6\ s^{-1}$, the line positions of the y components shift to the lower field and at the same time they broaden. Furthermore, in this region, the x and z lines at the $M_I = -1$ band also start to shift and become a broad singlet at $R_\perp = 1 \times 10^7\ s^{-1}$. Note that this value of $R_\perp = 1 \times 10^7\ s^{-1}$ is not enough to average out the x and y components at the $M_I = +1$ band.

These simulations do demonstrate how the subtle features of the slow-motional spectra are affected by the details of the motions. This will prove helpful in the next section.

Another important parameter affecting the predicted line shape of the slow-motional ESR spectra is the residual line width, $1/T_2^0$. In order to see the sensitivity to $1/T_2^0$ of the slow-motional spectra for anisotropic Brownian diffusion, we calculated theoretical spectra as a function of $1/T_2^0$ for several cases of $R_\parallel$ and $R_\perp$. It was found that the line shape changes considerably with a small variaion of $1/T_2^0$, especially in the slow-motional region of $R_\parallel$, $R_\perp \leq 1 \times 10^7\ s^{-1}$, which corresponds to our experiments. Thus, one has to be very careful in choosing $1/T_2^0$ to simulate the experimental spectra. The method we used will be discussed in the following section.

(D) Comparison between Experimental and Theoretical Spectra. (1) NO_2 on Vycor. The experimental spectra are compared in Figure 8 with the best simulations obtained with a Brownian diffusion model. We make the following points: (1) Below 42.2 K, the calculated spectra correspond fairly well to the experimental ones at the central band ($M_I = 0$), but they deviate considerably from

(40) R. F. Campbell, E. Meirovitch, and J. H. Freed, *J. Phys. Chem.*, 83, 525 (1979).

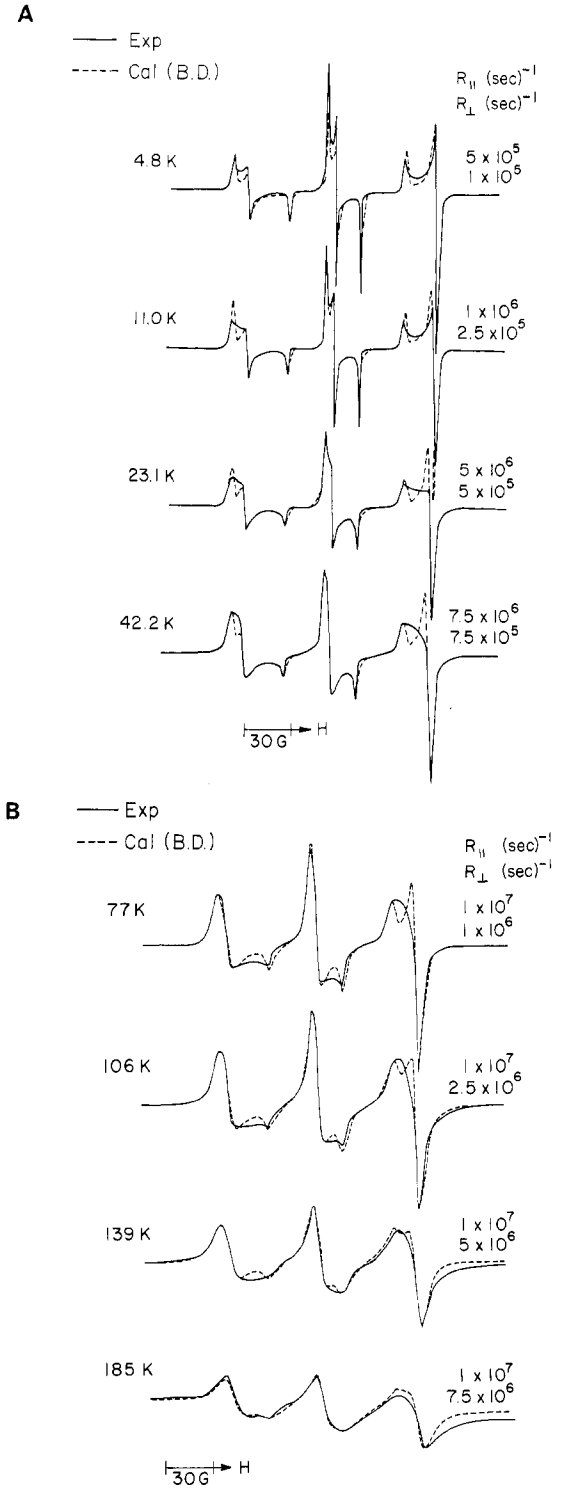

Figure 8. (A, B) The best-fitting theoretical spectra (Brownian rotational diffusion) compared with the experimental spectra of NO_2–Vycor in the temperature range between 4.8 and 185 K. The line widths used are given in Table II.

the experimental ones at the $M_I = \pm 1$ bands. Thus, the x and z components at the $M_I = \pm 1$ bands are collapsed into one broad line in the experimental spectra at 23.1 and 42.2 K, but they are still split in the calculated ones. Note that while the doublet (due to the x and z components) at the $M_I = \pm 1$ bands in the theoretical spectra can be averaged to one line by using higher values of $R_\parallel$, the fit to the relative peak heights at each of the M_I bands becomes worse. This disagreement cannot be improved by using any of the other models, as described below. (2) In

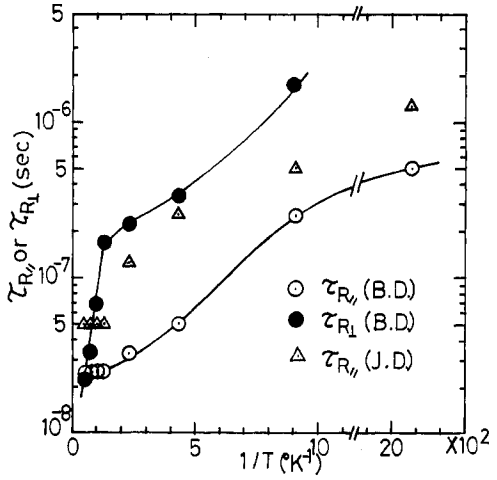

Figure 9. Plot of $\tau_{R\parallel}$ and $\tau_{R\perp}$ vs. $1/T$(K^{-1}) obtained by using the data in Table II. (The analysis based upon Brownian rotational diffusion.) The $\tau_{R\parallel}$ for jump diffusion ($R_\parallel \tau_\parallel = 1$) is given by Δ.

order to simulate the spectra, a broader $1/T_2^0$ was required with increasing temperature. For example, $1/T_2^0 = 1.0$ G was needed for the spectrum at 11.0 K, whereas $1/T_2^0 = 2.5$ G and $1/T_2^0 = 7.0$ G were required for the spectra at 77 and 185 K, respectively. The line widths used in the simulation are given in Table II together with the $R_\parallel$ and $R_\perp$ used. (Note that the theoretical spectra are not very sensitive to the $R_\parallel$ and $R_\perp$ so their precision is about ±50%). (3) The present simulations indicate that there are two distinct sets of spectra: i.e., those below 77 K and those above 77 K. Below 77 K, the rotational motion of NO_2 is quite anisotropic ($N \equiv R_\parallel/R_\perp \simeq 10$) with both $R_\parallel$ and $R_\perp$ increasing with temperature. At about 77 K, $R_\parallel$ reaches a plateau in its value, while $R_\perp$ increases from 1×10^6 s^{-1} (77 K) to 7.5×10^6 s^{-1} (at 185 K) with further increase in temperature. Thus, the rotational diffusion approaches isotropic motion above 77 K. These features are clearly seen in Figure 9. Also, for $T > 77$ K, the line width rapidly becomes broader while the total intensities of the spectra decrease sharply with temperture as mentioned previously. (4) Although the line shapes cannot be accurately reproduced, the components of the diffusion tensor, $R_\parallel$ and $R_\perp$, can be estimated from the theoretical spectra which give the same line positions as the experimental ones and are given in Table I.

We now discuss how we choose the value of $1/T_2^0$. In Figure 10 we show simulations carried out to fit the experimental spectrum recorded at 42.2 K. One sees that a change of $1/T_2^0$ from 1.0 to 3.0 G results in a considerable change in the relative peak heights at the $M_I = \pm 1, 0$ bands as well as in line shape. (Note that the maximum peak height of the theoretical spectrum is normalized to that of experimental one.) In the present studies, the $1/T_2^0$ giving the same spectral peak heights as those of the x and/or z components at the $M_I = \pm 1$ and 0 bands was considered the optimum choice, e.g., $1/T_2^0 = 2.0$ G is a good choice at 42.2 K, as seen in the figure. Indeed, this line width gives the best fit among the spectra calculated.

We next examine how the line shapes change with the orientation of the axis about which the motion occurs. We calculated spectra as a function of the polar and aximuthal angles (θ and ϕ) between the orientation of the principal coordinate system of the **g** and **A** tensors. We found from our calculations that the line shape is quite insensitive to the tilt angle, for $\theta \leq 45°$, in the range of $R_\parallel \simeq 1 \times 10^7$ s^{-1} and $R_\perp \simeq 1 \times 10^6$ s^{-1}. When spectra were calculated as a function of ϕ as well, sensitivity of the line shape was greater than in the case of only changing θ. However, the

TABLE II: Best-Fitting Parameters for Slow-Motional Spectra

T, K		$R_\parallel$, s^{-1}	$\tau_\parallel$, s	$R_\perp$, s^{-1}	$\tau_{R\parallel}$,[c]	$\tau_{R\perp}$,[d] s	$1/T_2^0$, G
4.8	BD[a]	5×10^5		$<1 \times 10^5$	5×10^{-7} ($N > 5$)[e]	$<1.7 \times 10^{-6}$	1.0
	JD[b]	1×10^6	1×10^{-6}	$<1 \times 10^5$	1.3×10^{-6}		
11.0	BD	1×10^6		$\leq 1 \times 10^5$	2.5×10^{-7} ($N \geq 10$)	$\leq 1.7 \times 10^{-6}$	1.0
	JD	2.5×10^6	4×10^{-7}	$\leq 1 \times 10^5$	5×10^{-7}		
23.1	BD	5×10^6		5×10^5	5×10^{-8} ($N = 10$)	3.3×10^{-7}	1.5
	JD	5×10^6	2×10^{-7}	5×10^5	2.5×10^{-7}		
42.2	BD	7.5×10^6		7.5×10^5	3.3×10^{-8} ($N = 10$)	2.2×10^{-7}	2.0
	JD	1×10^7	1×10^{-7}	1×10^6	1.3×10^{-7}		
77	BD	1×10^7		1×10^6	2.5×10^{-8} ($N = 10$)	1.7×10^{-7}	2.5
	JD	2.5×10^7	4×10^{-8}	2.5×10^6	5×10^{-8}		
106	BD	1×10^7		2.5×10^6	2.5×10^{-8} ($N = 4$)	6.7×10^{-8}	4.0
	JD	2.5×10^7	4×10^{-8}	5×10^6	5×10^{-8}		
139	BD	1×10^7		5×10^6	2.5×10^{-8} ($N = 2$)	3.3×10^{-8}	5.0
	JD	2.5×10^7	4×10^{-8}	1.0×10^7	5×10^{-8}		
185	BD	1×10^7		7.5×10^6	2.5×10^{-8} ($N = 1.3$)	2.2×10^{-8}	7.0
	JD	2.5×10^7	4×10^{-8}	1.5×10^7	5×10^{-8}		

[a] BD = Brownian diffusion. [b] JD = jump diffusion ($R_\parallel \tau_\parallel = 1$). [c] $\tau_{R\parallel} = 1/4R_\parallel$ for BD; $\tau_{R\parallel} = 5/4R_\parallel$ for JD. [d] $\tau_{R\perp} = 1/6R_\perp$ for BD. [e] $N \equiv R_\parallel/R_\perp$.

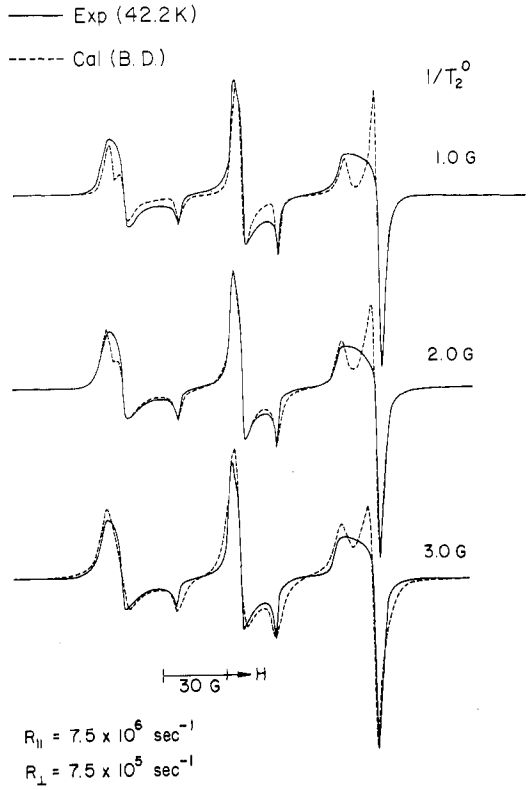

Figure 10. Theoretical spectra illustrating the sensitivity of slow-motional spectra (corresponding to the experimental spectrum at 42.2 K) of anisotropic Brownian rotational diffusion to the line width $1/T_2^0$ for $R_\parallel$ (parallel to y axis) = 7.5×10^6 s^{-1} and $R_\perp = 7.5 \times 10^5$ s^{-1}.

trends are found to be in the direction of worsening the agreement between experimental and theoretical spectra.

Theoretical spectra were calculated by using a moderate jump diffusion model ($R_\parallel \tau_\parallel = 1$)[25,29] and the best-fitting parameters are given in Table II. In contrast to the cases of O_2^-[29] and the nitroxide radicals,[25] the theoretical line shape was not significantly changed from that of Brownian diffusion, although the $R_\parallel$ obtained was different for the two models as seen from the table. The reason the line shape is not sensitive to the model is probably due to the particular values of the magnetic parameters for NO_2.

In fact, when $R_\parallel \tau_\parallel$ was varied from 0.1 (weak jump) to 10.0 (strong jump) keeping $\tau_{R\parallel}$ constant, no significant differences could be seen in the simulations. Thus, these jump models offer no significant improvement in the line shape over the use of a Brownian diffusion model (cf. Figure 8A). The same comments apply to the approximate free diffusion model.

(2) *NO_2 on Zeolite (Na-Zeolon).* We have already noted that for this case the 4.7 and 77 K spectra can be satisfactorily simulated as being in the rigid limit, i.e, frozen on the ESR time scale. Motional effects on the spectrum are observed for $T \gtrsim 120$ K. At 120 K, the NO_2 motion appears axially symmetric with the molecular y axis again the axis of faster motion, but the spectra become nearly isotropic with $R_\parallel \sim R_\perp$ 1×10^7 s^{-1} at ca. 250 K (based on a Brownian diffusion model). Also $1/T_2^0$ is already quite large at 250 K ($T_2^{0-1} \simeq 4$ G). No significant change of the line shape was observed for temperatures $T \geq 250$ K, but the intensity of the spectrum becomes weaker with increasing temperature, until it is no longer observable above 300 K.

IV. Discussion

We believe that our results for NO_2 dynamics on Vycor surfaces can best be understood in terms of two types of motions. The low-temperature motion (below 77 K) is dominated by anisotropic rotation of the NO_2 at a single surface site. The preferred axis for rotation is the molecular y axis. We estimate an "activation energy" (see below) for this motion to be $\approx 50 \pm 15$ cal/mol for both $\tau_{R\parallel}$ and $\tau_{R\perp}$ obtained from the Brownian rotational diffusion model. Above 77 K, the observed isotropic rotational motion is dominated by translational diffusion of the NO_2 to surface sites of different orientation (either by diffusion on the surface, or by gaslike "hops" between sites, or by collisions with N_2O_4, cf. discussion below). We estimate an activation energy for this process to be $\approx 0.5 \pm 0.1$ kcal/mol from $\tau_{R\perp}$ (which, according to our model, must be decreasing more rapidly with increasing T than $\tau_{R\parallel}$ until both τ_R's become equal by the translational mechanism). Such a low activation energy for the translational diffusion process appears consistent with our observation that the NO_2 is only weakly physisorbed to the Vycor surface. In the case of NO_2 on Na–zeolon, rotation about the y axis appears only by 120 K, but by 250 K the rotation appears as isotropic implying the translational mechanism sets in at much higher temperatures and is consistent with NO_2 being more strongly physisorbed than on Vycor.

This interpretation is consistent with the observation of significant intrinsic line broadening as the temperature is raised especially since the broadening becomes less pronounced for the Na–Zeolon support at lower temper-

atures. We suspect (in agreement with the suggestion by Lunsford[13]) that the exchange reaction

$$NO_2 + N_2O_4 \underset{k_3}{\overset{k_3}{\rightleftharpoons}} N_2O_4 + NO_2$$

may be a primary source of broadening. The loss in $[NO_2]$ adsorbed on the surface with increased temperature would imply that either dimerization to N_2O_4 is enhanced by increasing temperature and/or a reduced adsorption of NO_2 at the higher temperatures (which would be typical behavior).[36]

We have found that the higher temperature spectra on Vycor can be satisfactorily simulated by an exchange mechanism replacing the increasing intrinsic T_2^{-1}. We estimate an activation energy for such a process of about 0.4 ± 0.15 kcal/mol with an exchange rate of $(1.0 \pm 0.2) \times 10^8$ s^{-1} at 130 K. This activation energy is approximately the same as that obtained from the higher temperature rotational correlation times, and could imply that the NO_2, N_2O_4 exchange process is diffusion controlled.

This analysis implied that the exchange of NO_2 is with a species (e.g., N_2O_4) whose concentration remains substantially unchanged with temperature, or else one must correct the observed line broadening for the linear dependence of exchange on concentration. In the case of NO_2 on Vycor, if we assume a monolayer coverage of NO_2 and N_2O_4 on the surface, then even as $[NO_2]$ is decreasing substantially with increasing temperature, it may be that the combined effects of (diffusion controlled) dimerization and the chemical exchange lead to approximately constant numbers of particles on the surface with which NO_2 can interact. Clearly further work is required to understand these matters.

We do wish to point out that the NO_2, N_2O_4 exchange process could be an effective "translational-collision" mechanism for inducing what appears to be isotropic rotational reorientation.

Pietrzak and Wood[9] studied NO_2 on zeolites: Linde Type 10X (Ca^{2+} with ca. 9-Å channel size and Na^+ with ca. 10-Å channel size). These also required high NO_2 pressures (>250 mmHg) in order to get appreciable ESR signals consistent with our Na–Zeolon results. Their conclusion on the observed motional dynamics analyzed by the older Monte-Carlo method can in current terms be stated as characteristic of isotropic Brownian diffusion. It is likely that they were observing the translational-type of mechanism discussed above, but further study is called for.

We come now to the discrepancies between theoretical and observed ESR spectra at the lower temperatures. These discrepancies are somewhat similar to those we previously observed in our study of O_2^- adsorbed on Ti–Vycor surfaces, viz. the outer spectral lines in the slow-motional region were observed to be broader with unresolved detail compared to theoretical predictions.[29] The O_2^- spectrum is, however, just a **g** tensor, but the loss in detail for our NO_2–Vycor spectra relate to averaging of the g_x and g_z components. Thus it may be that a similar explanation, based on motional dynamics, could resolve the discrepancy for both cases. The possibilities mentioned for O_2^- that should be considered here are as follows: explicit inclusion into the model of a surface-induced potential barrier to reorientation of the NO_2 and/or inclusion of coupling of the NO_2 motions to surface modes, i.e., surface polarization effects due to the (van der Waals) interactions of NO_2 with a local surface site. Also, to the extent that the electronic structure of NO_2 is modified by the surface, and this modification is modulated by the reorientation of NO_2 on the surface, one should consider how the values of the components of the **g** and **A** tensors (in the molecular frame in which they are defined) might change as a function of the orientation of NO_2 relative to the surface. We discuss below the extent to which the surface does modify these tensors. Last of all we recall that in our classical models we did not consider inertial effects, because previous work has indicated that they would lead to a pronounced sharpening of spectral features, which is the opposite of our observed discrepancies.

It was also pointed out in our O_2^- study that it might be important to consider quantum mechanical effects on the motional dynamics of small molecules on the surface. These remarks are certainly appropriate for NO_2. The relevant gas-phase rotational constants, (i.e., $\mathcal{A}_i = \hbar^2/2I_i$) are well-known for NO_2 and are[12] 12.30 GHz (0.593 K) for $\mathcal{A}_x$, 239.9 GHz (11.56 K) for $\mathcal{A}_y$, and 13.00 GHz (0.626 K) for $\mathcal{A}_z$. These values, especially that for $\mathcal{A}_y$, are much larger than the **g** and **A** tensors, so that a low-pressure gas-phase spectrum, even in magnetic fields of 3 kG and at 9-GHz frequencies, is dominated by the "quantum-mechanical averaging" of the **g** and **A** tensor anisotropies along lines we have already outlined for the simpler case of O_2^-. Also, the high-pressure, averaged ESR spectrum of gaseous NO_2 is well-known to be a simple triplet (with spacing of 132 MHz).[41] Neither of these two limits is appropriate for the analysis of NO_2 surface spectra, especially those observed at low temperature, which are (nearly) rigid-limit results.

Instead, we proposed in our O_2^- work that one should rewrite the quantum mechanics for rotational motion in terms of a "renormalized" moment of inertia tensor: $\tilde{\mathbf{I}}$ (and a corresponding $\tilde{\mathcal{A}}$) as well as an effective potential $V(\Omega)$ in terms of the Euler angles Ω relating the orientation of the principal axes of inertia of NO_2 relative to the surface so that the rotational motion is described by an effective Hamiltonian yielding

$$\sum_{i=x,y,z} \frac{L_i^2}{2I_i}\Psi + V(\Omega)\Psi = E\Psi$$

in the absence of thermal relaxation with L_i the ith component of the angular momentum operator. In order to illustrate how significantly the interaction with the surface must modify the gas-phase constants we first consider the case of $V(\Omega) \approx 0$, so the surface motion is free. Let us also consider just rotation about the molecular y axis since this corresponds to a very small moment of inertia (see above) and is the primary motion observed at low temperatures. In order to prevent complete quantum mechanical averaging of A_x with A_z and g_x and g_z we require a much increased $\tilde{I}_{yy}$ (or decreased $\tilde{\mathcal{A}}_{yy}$). Since $g_x - g_y$ is the smaller, we require, in order that these components not be averaged for the $M_I = 0$ band at 4.8 K that $\tilde{\mathcal{A}}_{yy} < \beta_e B_0(1/4)|g_x - g_y| \approx 4.5 \times 10^{-4}$ K, or $\tilde{\mathcal{A}}_{yy}$ must be *at least* 10^4 times smaller than $\mathcal{A}_{yy}$! If we introduce a large barrier $V(\phi)$ to rotation about the molecular y axis, then we would only require that Δ_0, the "tunneling" splitting of torsional sublevels of the ground torsional level, obeys $n|\Delta_0| < I_2(1/2)(3/2)^{1/2}$ (for $V_n(\phi) \propto \cos n\phi$). This may be more reasonable physically, although no ESR spectral evidence has been obtained for the classical-limiting model of coherent n-fold rotational jumps (cf. ref 26).

Either limiting surface quantum mechanical model could "explain" the residual motional effects detected at 4.8 K for NO_2–Vycor. In the case of free motion but a greatly reduced $\tilde{\mathcal{A}}_{yy}$ there would be many thermally accessible

(41) J. G. Castle, Jr., and R. Beringer, *Phys. Rev.*, **80**, 114 (1950).

rotational J levels each with its own effective $(g_x - g_z)$ and $(A_x - A_z)$ (actually the situation is even more complex, cf. ref 29), so there would be *inhomogeneous* broadening of the respective spectral regions. In the case of strongly hindered motion, Δ_0 would be very sensitive to local variations in surface-induced potential $V(\phi)$, and this can lead to site-to-site variation in apparent $(g_x - g_z)$ and $(A_x - A_z)$.[29] Again this would be inhomogeneous broadening. The distinction between inhomogeneous vs. homogeneous broadening can, in principle, be made with electron spin-echo experiments and preliminary results do appear to be consistent with an inhomogeneous mechanism.[42]

The higher temperature onset of thermal relaxation can also be analyzed from a quantum mechanical approach.[29] In summary, our point of view is that the ESR spectra are much closer to those characteristic of classical models than of gaslike quantum models, so that quantum corrections, if required, must be relatively small.

On the other hand, we do note that observations made by Brailsford and Morton[21] on NO_2 in alkali-halide crystals and Bojko and Silsbee[22] on NO_2 in KCl showed quantum mechanical averaging about the molecular y axis even at 2 K. This is necessarily due to a vacancy site in the crystal with little effective rotational hindrance about this axis from the crystal potential. Our results for surface NO_2–vycor are not of this type, although these previous observations suggest the possible importance of residual quantum effects. Bojko and Silsbee[22] find that the spin-rotational coupling is important in analyzing their ESR spectrum, but it is significantly reduced from the free molecule value probably due to the hindering potential. We now wish to consider any residual effects of the spin-rotational coupling on the surface NO_2–vycor.

The spin-rotational interaction may be written as $\mathbf{J}\cdot\mathbf{C}\cdot\mathbf{S}$ where $\mathbf{C}$ is the spin-rotational coupling tensor which is quantized in the molecular frame (x, y, z) and is accurately known for gaseous NO_2.[12] In the limiting case where only rotation about the molecular y axis is allowed it becomes $J_y C_{yy} S_y$ with $C_{yy} = 5.412$ GHz for the gas molecule, clearly a large interaction for 9-GHz spectroscopy. The dominant portion of $\mathbf{C}$ is known to result from the second-order perturbation cross term between the spin–orbit coupling $\lambda\mathbf{L}\cdot\mathbf{S}$ and the electronic orbit-rotational coupling $\mathbf{L}\cdot\boldsymbol{\mathcal{A}}\cdot\mathbf{J}$, which leads to the relation $\mathbf{C} \approx -2\Delta\mathbf{g}$ where $\Delta\mathbf{g} = \mathbf{g} - g_e\mathbf{1}$. [In fact $(g_{yy} - g_e) = -0.0113$ while $-C_{yy}/2\mathcal{A}_{yy} = -0.01128$ for the gas molecule, or especially good agreement.][43] If we use the limiting surface model of a free rotor ($\psi_m = 1/(2\pi)^{1/2}e^{im\phi}$) with renormalized $\tilde{\mathcal{A}}$, then the free rotor states will have a diagonal contribution: $m\tilde{C}_{yy}\cos\theta S_z$ (and nonsecular term: $m\tilde{C}_{yy}\sin\theta S_z$) where θ is the angle between the lab z and molecular y axis. However, we must use a reduced $\tilde{C}_{yy} \approx -2\Delta\mathbf{g} \lesssim 0.2$ MHz (or 1×10^{-5} K) due to the surface renormalization of $\tilde{\mathcal{A}}$, and it becomes of negligible importance to the ESR spectrum. In a similar manner, one may consider the other limiting case of a highly hindered rotor (i.e., a large $V_n\tilde{I}/2\hbar^2$). Here $J_y C_{yy} S_y$ can only connect different torsional levels separated by $\Delta E_v \approx n\hbar(V_n/2\tilde{I})^{1/2}$ (since $J_y = -i\hbar(\partial/\partial\phi)$), so it will be unimportant for $V_n(\phi)$ very large. Also, the secular term (which must be at least as important as the nonsecular term) is unimportant for $\theta \approx \pi/2$, which corresponds to the excessively broadened x and z components.

Finally, we note that the spin-rotation mechanism is independent of nuclear-spin quantum number, so that it cannot explain the low temperature discrepancies most prominent for the $M_I = \pm 1$ bands.[44]

It would be of interest to know the orientation of the NO_2 on the surface, i.e., is the molecular y axis perpendicular or parallel to the surface, when rotation is largely about the y axis? Based upon our results we favor the parallel orientation. This is because the y axis perpendicular to the surface (i.e., NO_2 "standing-up" but weakly bonded via a single oxygen atom) would present a minimum of surface hindrance to reorientation about this axis (viz. only a small increse in I_{yy}) while for y parallel to the surface there should be considerable interference of the surface with the motion, since a rotation about ϕ would alternately bring NO_2 flat on the surface and either the N atom or the two O atoms nearer the surface. Thus, for the perpendicular orientation a gaslike rotation would be expected and is contrary to our above discussion, while for a parallel orientation that motion is likely to be dominated by surface interactions and is more consistent with our discussion.

Clearly studies with ^{17}O-labeled NO_2 would be helpful[45] in distinguishing the two possibilities (Brailsford and Morton[21] did find equivalent ^{17}O's for NO_2 in KCl) as would studies on oriented single-crystal surfaces.

We note that Iwaisumi et al.[11] have observed similar temperature-dependent ESR line shapes for NO_2 adsorbed on a silica gel surface *above* 77 K, and they concluded from their axially symmetric $\mathbf{A}$ and $\mathbf{g}$ tensors at 77 K that NO_2 rotates about the y axis, consistent with our observation. They infer from this that y is perpendicular to the surface, since that would allow rotation about this axis. Our analysis, as we have discussed, suggests that the motion would then be too unrestricted! There is, in fact, some indirect evidence for a preferential orientation of NO_2 such that the plane of the molecule is parallel to the surface. Kasai et al.[8] have found that when NO_2 is trapped in a Neon matrix at 4 K formed by depositing the neon on a flat rod, the NO_2 tends to align parallel to the surface. They suggest that the surface of the oriented matrix might "dictate the orientation of planar molecules impinged upon it." If we compare the $\Delta A_i \equiv A_i - a_{iso}$ given in Table I for neon matrix vs. the gas (for which $\Delta A_x \approx \Delta A_y$) then we find ΔA_y remains virtually unchanged while ΔA_x and ΔA_z are reduced in magnitude from −18.7 to −3.4 MHz (for A_x) and from +38.5 to 24.4 MHz (for A_z). We take this as the effect of van der Waals forces of the neon layers above and below

(42) L. J. Schwartz, M. Shiotani, A. E. Stillman, and J. H. Freed, unpublished.

(43) R. F. Curl, *J. Mol. Phys.*, **9**, 585 (1965).

(44) The effect of spin rotation in the "classical" limit may also be considered. It seems appropriate to consider a model of slow rotational reorientation, but where angular momentum relaxation can still occur. In the case of unhindered axial rotation about the molecular y axis the expressions of Goldman et al. [*J. Chem. Phys.*, **59**, 3071 (1973)] become

$$T_2^{-1SR} = T_2^{-1}(sec)^{SR} + \tfrac{1}{2}T_1^{-1SR}$$

$$T_2^{-1}(sec)^{SR} = \frac{kT}{\hbar^2}\tilde{I}_y\tilde{C}_{yy}\cos^2\theta\tau_{Jy}$$

$$T_1^{-1SR} = \frac{2kT}{\hbar^2}\tilde{I}_y\tilde{C}_{yy}\sin^2\theta\tau_{Jy}(1 + \omega_0^2\tau_{Jy}^2)^{-1}$$

which are seen to be independent of $\tilde{I}$ for a Brownian model where the angular momentum relaxation time $\tau_{Jy} = \tilde{I}_{yy}/\xi_y$ with ξ_y the friction coefficient [provided $\omega_0^2\tau_{Jy}^2 \ll 1$ or else $\omega_0^2\tau_{Jy}^2 \gg 1$ so $T_1^{-1SR} \ll T_2^{-1}(s)^{SR}$]. Again we see that $T_2^{-1}(s)^{SR}$ can only significantly broaden the y components of the spectrum and T_2^{-1SR} is nuclear spin independent, both inconsistent with "explaining" our discrepancies. [Note also, the quantum-classical correspondence for spin-rotational relaxation has yet to be fully explored]. However, the M_I independence of T_2^{-1SR} is not inconsistent with the higher temperature broadening observed, which we believe is more likey due to chemical or spin exchange.

(45) Preliminary efforts using NO_2 prepared from $N^{16}O$ and O_2 enriched with approximately 20% ^{17}O yielded a spectrum with broader widths and no ^{17}O hfs could be clearly distinguished at 77 K. It seems clear that NO_2 highly enriched with ^{17}O should be used in any future work.

the NO_2 plane. For NO_2–vycor, ΔA_y is again virtually unchanged while $\Delta A_x = -18.7$ and $\Delta A_z = +32.8$, or the same trends as for neon but less pronounced. This is to be expected for NO_2 above the surface rather than sandwiched between layers. (We note that the molecular orbital analyses[15-17] rely on configuration interaction to interpret the inequality of $\Delta A_x \neq \Delta A_y$ induced by the medium.) Last of all, we wish to comment that, as the NO_2 rotates about the y axis above the Vycor surface, one may anticipate that **A** (and **g**) may be modulated by interaction with the surface (as we noted above).

In fact, one might envision a cooperative rotation of the NO_2 about its y axis with a small bond angle variation[33] with the rotation and with a small variation in the distance of its center of mass from the surface in order to accommodate this motion. Finally, one may speculate on a surface structure in which both oxygens have weak van der Waals bonds to the surface, which could allow a partial rotation of the NO_2 about its y axis to include the two conformers in which the NO_2 plane is parallel to the surface and the conformer in which the oxygens point to the surface, while at the same time suppressing rotation about the molecular x and y axes. (Note that a 180° rotation about ϕ is sufficient to average out second-rank tensor components $g_x - g_y$ and $A_x - A_y$, cf. ref 29.) This should be the subject of further investigation.

V. Conclusions

The NO_2 molecule adsorbed on Vycor displays a predominantly axial rotation about the y axis (parallel to the O–O internuclear axis) below 77 K but above this temperature the motion becomes more nearly isotropic probably due to a translational diffusion mechanism. The line shape analysis is reasonably consistent with this picture, except for some discrepancies in detail for 77 K and below, which are worthy of further study. From consideration of quantum models for the rotation, it is suggested that this y axis aligns parallel to the surface, but further work with ^{17}O labeling is recommended.

Acknowledgment. We thank Dr. G. Moro and Ms. L. Schwartz for their help and advice. This research was supported by Grant No. DE-AC02-80ER04991 from the Office of Basic Energy Sciences of the DOE, by NSF Grant CHE 80-24124, and by the Cornell Materials Science Center (NSF), and acknowledgment is made to the donors of the Petroleum Research Fund, administered by the American Chemical Society, for partial support.

Temperature and Density Dependence of the Proton Lifetime in Liquid Water

W. J. Lamb, D. R. Brown, and J. Jonas*

Department of Chemistry, School of Chemical Sciences and Materials Research Laboratory, University of Illinois, Urbana, Illinois 61801
(Received: June 22, 1981)

The NMR $T_{1\rho}$ technique is developed to determine the average residence time, τ_e, of a proton on a water molecule in liquid water. The temperature and density dependence of τ_e is measured in the range 0–100 °C and at densities up to 1.125 g cm^{-3} (pressure range, 1 bar to 5.6 kbar). The $T_{1\rho}$ technique is compared to other NMR methods such as the T_1 and T_2 techniques also used to determine τ_e. The anomalous behavior of τ_e with compression at temperatures below 40 °C parallels changes in other physical properties of liquid water.

Introduction

Ever since Meiboom's original paper,[1] there has been considerable effort to determine the rate constants governing proton transfer between H_3O^+ (k_1) and OH^- (k_2) ions and neutral water molecules. However, a review of the literature[2-6] since 1961 reveals that the values of k_1 and k_2 and the corresponding activation energies for these rates are still in dispute. More recently, work has centered on the measurement of the average time that a proton spends on a water molecule (τ_e) in bulk neutral water and in occluded water. Woessner[7] has measured τ_e's for preferentially ordered water molecules in minerals and porous clays. Pintar et al.[8] have determined τ_e values for bulk neutral water from NMR spin–spin relaxation (T_2) measurements, and Noack et al.[9] have determined τ_e by using the field-cycling technique to measure spin–lattice relaxation (T_1) at very low H_0 fields. In this work we present the first direct application of NMR spin–lattice relaxation measurements in the rotating frame ($T_{1\rho}$) to determine the temperature and density dependence of τ_e.

Meiboom[1] has shown that the Bloch equations modified for proton exchange may be solved provided certain assumptions are made. For our experimental conditions these assumptions are valid, and the expression relating the proton lifetime to the difference in relaxation rates is

$$\frac{1}{T_{1\rho}} - \frac{1}{T_1} = \tau_e \sum_i \frac{P_i \delta_i^2}{1 + \tau_e^2(\delta_i^2 + \omega_1^2)} \qquad (1)$$

where τ_e is the average time that a proton is bonded to a given oxygen atom, P_i is the relative intensity of the ith

(1) S. Meiboom, *J. Chem. Phys.*, **34**, 375 (1961).
(2) A. Loewenstein and A. Szöke, *J. Am. Chem. Soc.*, **84**, 1151 (1962).
(3) Z. Luz and S. Meiboom, *J. Am. Chem. Soc.*, **86**, 4768 (1964).
(4) R. E. Glick and K. C. Tewari, *J. Chem. Phys.*, **44**, 546 (1966).
(5) S. W. Rabideau and H. G. Hecht, *J. Chem. Phys.*, **47**, 544 (1967).
(6) D. L. Turner, *Mol. Phys.*, **40**, 949 (1980).
(7) D. E. Woessner, *J. Magn. Reson.*, **16**, 483 (1974).
(8) R. R. Knispel and M. M. Pintar, *Chem. Phys. Lett.*, **32**, 238 (1975).
(9) V. Graf, F. Noack, and G. J. Bénê, *J. Chem. Phys.*, **72**, 861 (1980).

0022-3654/81/2085-3883$01.25/0